Plasma Capacitor with Ion Acoustic Waves

F. Leuterer

Max-Planck-Institut für Plasmaphysik, 8046 Garching, Germany

(Z. Naturforsch. **29 a**, 851–858 [1974]; received April 5, 1974)

We examine experimentally and theoretically the r. f. potential within a capacitor, filled with a homogeneous plasma in a magnetic field and driven at frequencies $\omega_{ci} < \omega < 4\,\omega_{ci}$. We assume the ions to be cold, and the electrons to have a Maxwellian velocity distribution along the magnetic field, but zero radius of gyration. Thus ion acoustic waves are included. The whole k_z-spectrum of the exciter is needed to explain the experimental results.

I. Plane Wave Dispersion Relation in an Infinite Homogeneous Plasma

In an actual laboratory plasma experiment at ion wave frequencies the geometrical dimensions of the arrangement are often much smaller than the free space wavelength of the applied signal. Therefore we will use an electrostatic analysis to describe the wave propagation in the plasma. The dispersion relation then generally is, if we set $k_y = 0$,

$$k_x^2 K_{xx} + k_z^2 K_{zz} = 0 \tag{1}$$

with

$$K_{xx} = 1 + \pi_{xxe} + \pi_{xxi}\,; \quad K_{zz} = 1 + \pi_{zze} + \pi_{zzi}\,. \tag{1 a}$$

K is the dielectric tensor, $\boldsymbol{\pi}$ is the polarization tensor [1] and the subscripts e and i describe the contributions due to electrons or ions. In (1 a) we have neglected the magnetization tensor since in an electrostatic calculation the contribution of it vanishes identically. In a hot plasma we have

$$\pi_{xx} = \frac{\omega_p^2}{\omega\,\omega_c}\,\frac{e^{-\mu}}{\mu}\,\xi_0 \sum_{-\infty}^{+\infty} n\, I_n(\mu)\, Z(\xi_n) \tag{2}$$

and

$$\pi_{zz} = -\frac{\omega_p^2}{\omega^2}\, e^{-\mu}\, \xi_0^2 \sum_{-\infty}^{+\infty} I_n(\mu)\, Z'(\xi_n) \tag{3}$$

with

$$\mu = k_x^2 R^2; \quad \xi_n = \frac{\omega - n\,\omega_c}{\sqrt{2}\, k_z\, v_{th}}\,,$$

and the other symbols have their usual meaning.

In this paper we assume not only $\omega \ll \omega_{ce}$ but a magnetic field strong enough that we may consider it as infinitely strong with respect to the electrons, i. e. $\omega_{ce} = \infty$ and $\mu_e = 0$. In this case the electron polarization terms become:

$$\pi_{xxe} = 0; \quad \text{and} \quad \pi_{zze} = -\,(\omega_{pe}^2/\omega^2)\,\xi_{oe}^2\, Z'(\xi_{oe})\,. \tag{4}$$

The ion polarization terms remain as given by (2) and (3). Depending on the ratio of the phase velocity parallel to the magnetic field ω/k_z and the thermal velocity of the electrons v_{the} (assuming $v_{thi} \ll v_{the}$), we may use various approximations:

a) $\quad v_{the} \ll \omega/k_z \quad$ or $\quad \xi_{oe} = \dfrac{\omega}{\sqrt{2}\, k_z\, v_{the}} \gg 1\,.$

Here we can use the asymptotic expansion for the plasma dispersion function. This applies essentially for the case $k_z \to 0$, i. e. strictly perpendicular propagation. The dispersion relation in this case then is

$$k_x^2 (1 + \pi_{xxi}) + k_z^2 (1 - \omega_{pe}^2/\omega^2) = 0\,. \tag{5}$$

For cold ions this is:

$$k_x^2 = -\,k_z^2\, \frac{1 - \omega_{pe}^2/\omega^2}{1 - \omega_{pi}^2/(\omega^2 - \omega_{ci}^2)}\,. \tag{5 a}$$

Out of (5) for $k_z = 0$ we get the ion-Bernstein wave dispersion relation

$$k_x^2 (1 + \pi_{xxi}) = 0\,. \tag{5 b}$$

b) $v_{thi} \ll \omega/k_z \ll v_{the}$; or $\xi_{oe} \ll 1$; but all $\xi_{ni} \gg 1$. Here we use the power series expansion for the plasma dispersion function, which, taking only the first term, yields the dispersion relation:

$$k_x^2 (1 + \pi_{xxi}) + k_z^2 (1 + 2\,\omega_{pe}^2/\omega^2\, \xi_{oe}^2 + \pi_{zzi}) = 0\,. \tag{7}$$

For $k_z^2 \ll k_x^2$ we may neglect $(1 + \pi_{zzi}) \cdot k_z^2$ and get

$$\mu_i (\omega_{ci}^2/\omega_{pi}^2)\,(1 + \pi_{xxi}) + T_i/T_e = 0$$

or

$$k_x^2 (1 + \pi_{xxi}) \cdot \frac{\varkappa T_e}{M}\,\frac{1}{\omega_{pi}^2} + 1 = 0\,. \tag{7 a}$$

Reprint requests to Dr. S. Witkowski, Max-Planck-Institut für Plasmaphysik, *D-8046 Garching* bei München.

Compared with (5 b) we see that (7 a) contains an additional constant, 1. This has the effect that the solution $k_x = 0$ of Eq. (5 b) is now shifted to a solution $k_x \neq 0$, which is a forward wave existing in a dense plasma in addition to the backward Bernstein waves.

Taking the limit of cold ions, i. e. $\pi_{xxi} = -\omega_{pi}^2/(\omega^2 - \omega_{ci}^2)$, we can extract this wave out of (7 a) and get:

$$k_x^2 = \frac{\omega^2}{\varkappa T_e/M} \frac{\omega^2 - \omega_{ci}^2}{\omega_{pi}^2 + \omega_{ci}^2 - \omega^2} \frac{\omega_{pi}^2}{\omega^2}, \quad (7\,b)$$

which we recognize as an ion acoustic wave propagating almost perpendicular to the magnetic field. It is the wave which in Stix's book [2] is called the electrostatic ion cyclotron wave. In order to get Eq. (7 b) we made the assumptions $\omega/k_z \ll v_{the}$ and also $k_z^2 \ll k_x^2$. For larger k_z the second condition does not hold. Then the term $k_z^2(1 + \pi_{zzi})$ in Eq. (7) is no longer negligible. The dispersion equation then becomes

$$k^2 = k_x^2 + k_z^2 = \frac{\omega^2}{\varkappa T_e/M} \cdot \frac{\omega_{pi}^2(\omega^2 - \omega_{ci}^2)}{\omega_{pi}^2(\omega^2 - \omega_{ci}^2 \cos^2\Theta) - \omega^2(\omega^2 - \omega_{ci}^2)}. \quad (7\,c)$$

Θ is the angle between $\boldsymbol{k}$ and $\boldsymbol{B}_0$.

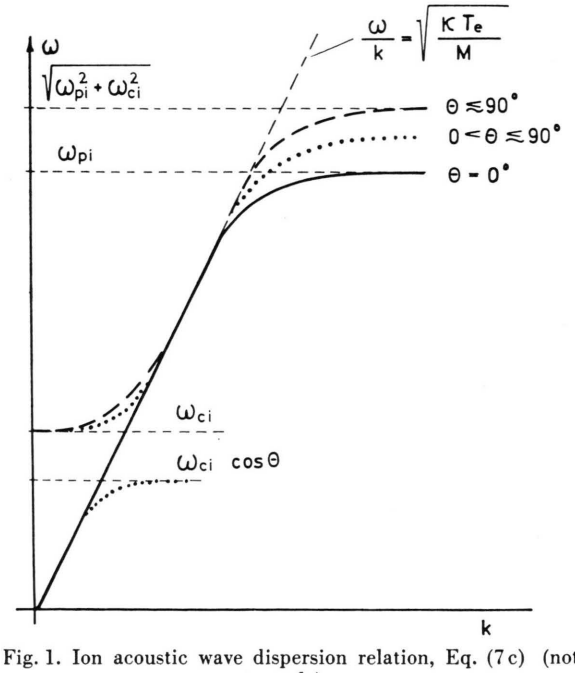

Fig. 1. Ion acoustic wave dispersion relation, Eq. (7 c) (not to scale).

A dispersion diagram corresponding to Eq. (7 c) is shown in Figure 1. Note, that in taking $\omega_{ce} \to \infty$, the lower hybrid frequency becomes $\omega_{LH}^2 = \omega_{pi}^2 + \omega_{ci}^2$, and Fig. 1 applies only as long as this relation holds, i. e. for $\omega_{pi}^2/\omega_{ci}^2 \lessapprox 200$. Care must also be taken if ω approaches ω_{LH}, since at larger k-values we may arrive at the point where $k_x^2 \cdot R_i^2 = \mu_i$ is no longer small enough that ion temperature effects are negligible. Dispersion measurements of the waves shown in Fig. 1 have been made by Hirose et al. [3].

Equation (7 a), compared to (7 b), also includes ion temperature effects and has been evaluated by Ault et al. [4] and also by Schmitt [5]. Their dispersion characteristics show, how the ion Bernstein waves, Eq. (5 c), join onto the perpendicular ion acoustic waves Eq. (7 b) and a gap appears in the frequency range below a harmonic $n\,\omega_{ci}$. Such a dispersion diagram is shown in Figure 2. Here we see that the coincidence of the forward wave branch of Eq. (7 a) and the perpendicular ion acoustic waves, Eq. (7 b) is very good for $\omega^2 \ll \omega_{LH}^2$ and for small values of T_i/T_e. With increasing T_i/T_e the gap width increases and the features of the perpendicular ion acoustic wave disappear. This is due to the fact that μ_i increases and ion temperature effects become serious.

c) In the range $v_{thi} \ll \omega/k_z \approx v_{the}$ we cannot use any approxamtion for $Z'(\xi_{oe})$ and we have to use the full dispersion relation

$$k_x^2(1 + \pi_{xxi}) + k_z^2(1 + \pi_{zzi} + \pi_{zze}) = 0.$$

This yields for cold ions

$$k_x^2 = -k_z^2 \frac{1 - \omega_{pi}^2/\omega^2 - \omega_{pe}^2/\omega^2\,\xi_{oe}^2\,Z'(\xi_{oe})}{1 - \omega_{pi}^2/(\omega^2 - \omega_{ci}^2)}. \quad (8)$$

II. Capacitor Experiment

With this experiment we want to look for a manifestation of the waves described above. The plasma used is produced in helium at about 3×10^{-3} Torr by a beam of electrons, $U \approx 60$ V, which penetrate a $\approx 90\%$ transparent anode grid. The electron current was controlled with a grid between the cathode and the anode. After a length of about 70 cm the plasma, diameter ≈ 5 cm, was terminated by a collector plate which had the same potential as the anode grid. Superimposed was a magnetic field $B_0 \approx 500 \div 700$ Gauss. The density has been determined by measuring the dispersion character-

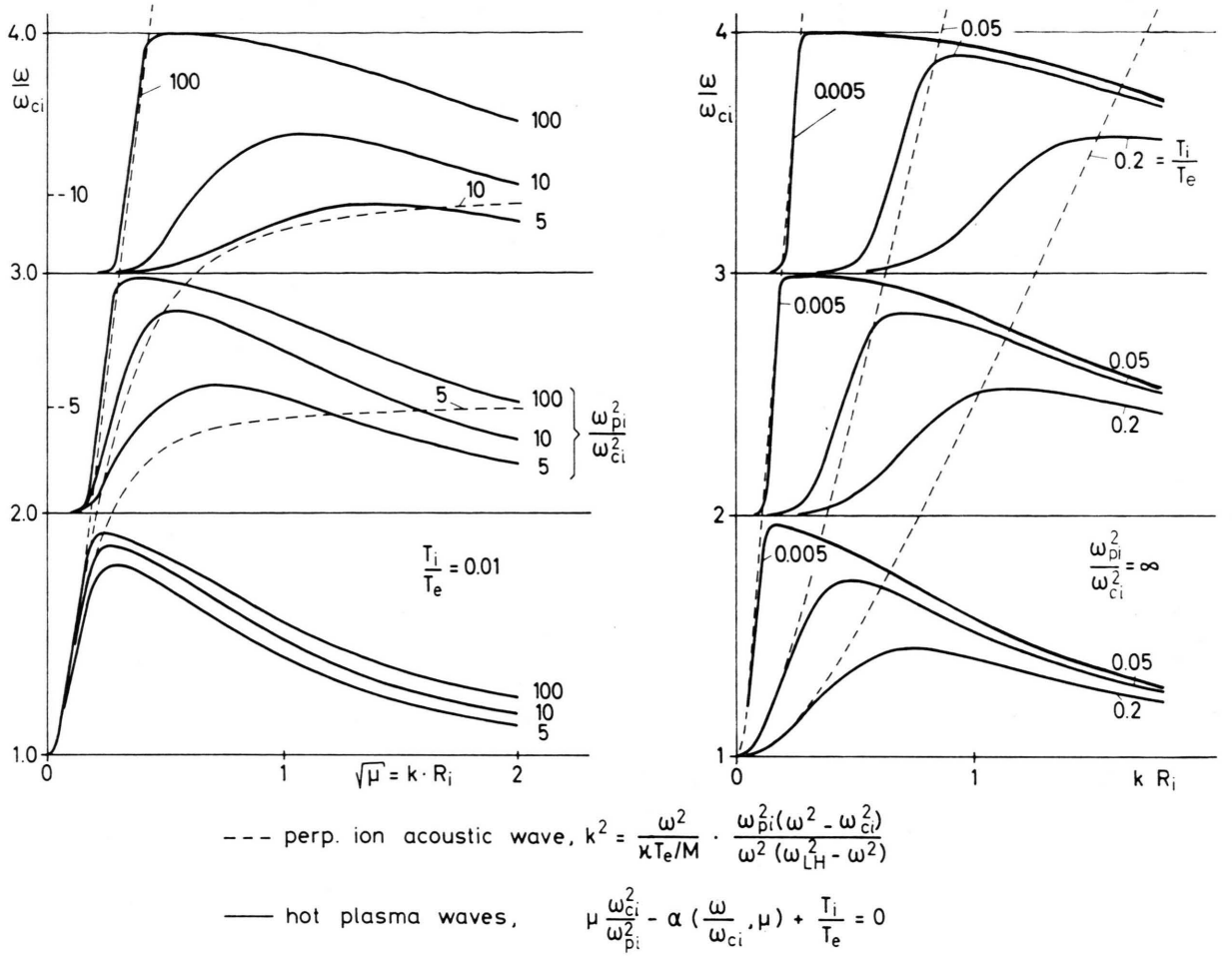

Fig. 2. ——— hot plasma dispersion relation, Eq. (7a), – – – perpendicular ion acoustic wave, Eq. (7b)
a) $T_i/T_e = 0.01$, different densities, b) $\omega_{pi}^2/\omega_{ci}^2 = \infty$, different T_i/T_e.

istics of the electron plasma waves joining on to the Trivelpiece-Gould mode [6] ($f = 80 \div 200$ MHz). For a cathode current of $i_c = 50$ mA we got $n_e = (4.5 \pm 1) \times 10^8$ cm^{-3}. The electron temperature was determined with ion acoustic waves ($f = 80 \div 150$ kHz) propagating parallel to the magnetic field and was found to be $T_e \approx 3$ eV.

The waves are excited by driving an r. f. current through a plasma filled capacitor formed by two shells on opposite sides of the plasma column, Figure 3. For the r. f. measurements (400 – 1000 kHz) we used a polar interferometer [7] to display the measured r. f. potential as $\Phi(x) = \Phi_0(x) \cdot e^{i\varphi(x)}$ in

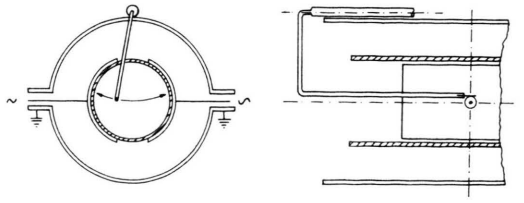

Fig. 3. Experimental arrangement.

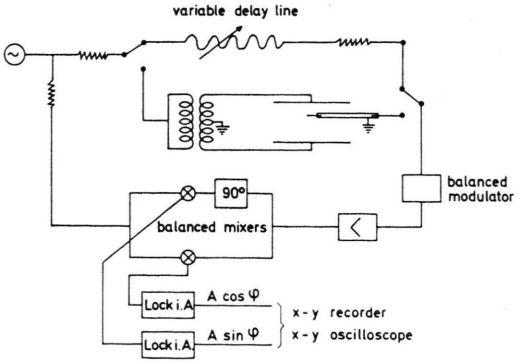

Fig. 4. Interferometer circuit.

the complex plane. A block diagram of this arrangement is shown in Figure 4.

Observing the signal sent through the delay line rather than through the plasma we can determine the sense of rotation of the vector in the complex plane indicating a forward wave. Increasing the signal path length by increasing the delay is equivalent to moving the detector in the direction of the phase velocity of the forward wave on the delay line. Result: a clockwise sense of rotation indicates a forward wave.

Experimentally obtained records of the r.f. potential in the plasma are shown in Figure 5. How can we interprete such a trace? 1. the presence of loops, i.e. of a phase variation $\varphi(x)$, tells us that we have waves in the plasma. 2. the centers of these loops don't coincide with one another and also not with the origin of the complex plane; therefor the wave signal is superimposed on some other signal. 3. moving along the trace, i.e. when the probe moves from one capacitor plate through the plasma to the other plate, we see that the sense of rotation with which these loops are described changes at the point where the probe is in the center of the plasma. This tells us that we have radially propagating waves. 4. the sense of rotation itself tells us that the phase velocity of these waves is directed from the capacitor plates towards the center of the plasma column.

Near the center of the plasma, where the sense of rotation changes, the trace is a piece of a straight line going roughly through the origin and thus represents nearly only amplitude variation but not a phase variation, i.e. the features of a standing

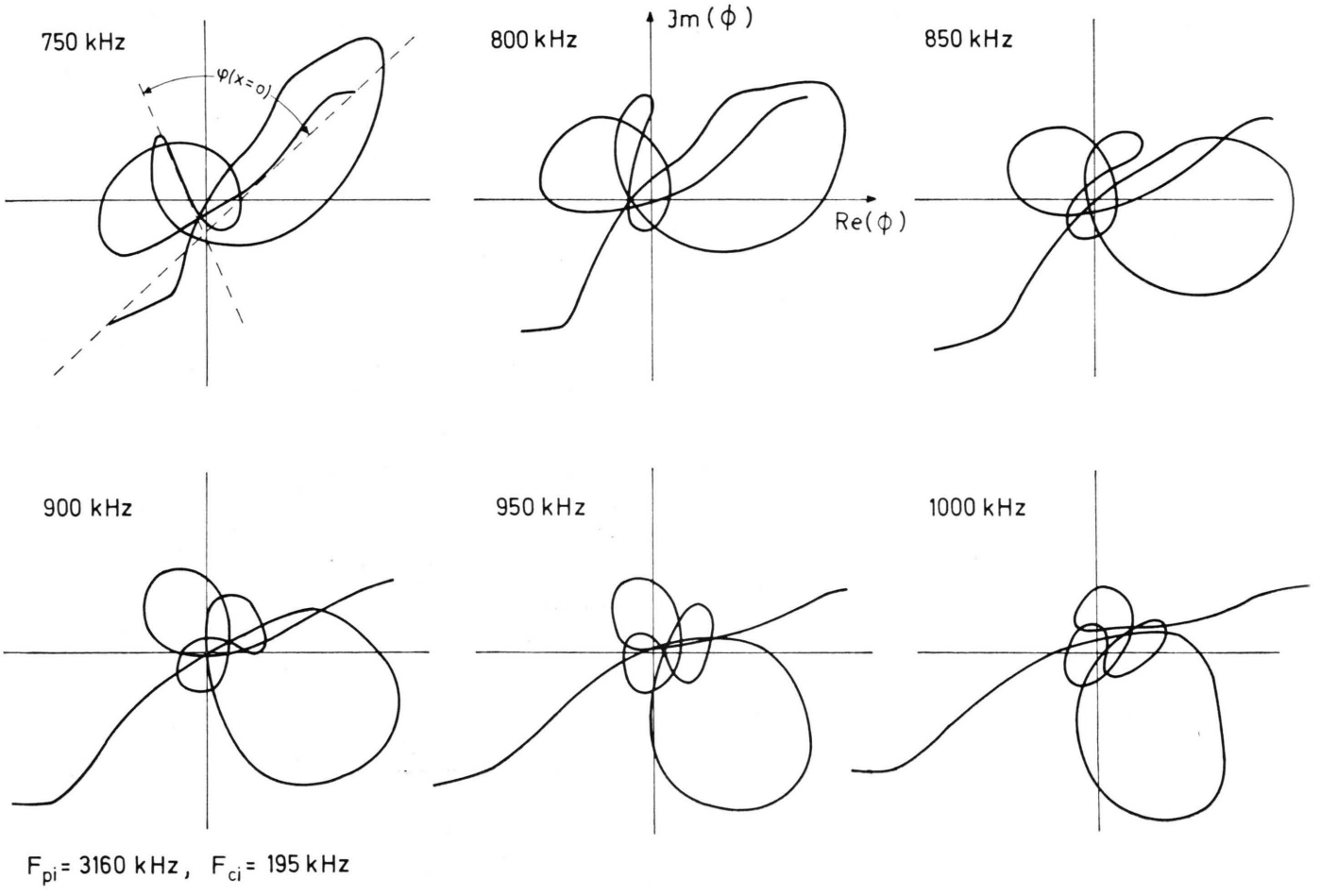

Fig. 5. Experimental r.f. potentials in the complex plane for different frequencies. $f_{pi} = 3160$ kHz, $f_{ci} = 195$ kHz.

wave pattern. We consider now the angle of this piece of straight line in the complex plane. In Fig. 5 we see how this angle changes clockwise with frequency. There is, in a wide parameter range, nearly no such change observeable when the density or the magnetic field are varied. The wavelength of the waves we see can be roughly determined by measuring the distance which the probe moves in describing one full loop and lies between 1 and 3 cm.

All the above observations lead us to the assumption that the waves observed are rather the perpendicular ion acoustic waves, Eq. (8), and not the backward ion Bernstein waves.

With this in mind we are tempted to describe what we see as a superposition of an ion acoustic wave potential superimposed on a cold plasma potential (which has an infinite wavelength), the wave potential being due to two damped waves travelling

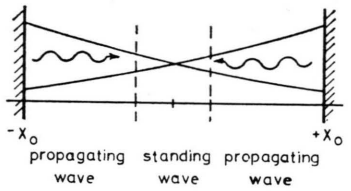

Fig. 6. Superposition of two radially propagating damped waves.

from the two plates into the plasma and forming the standing wave pattern in its center, Figure 6. If this is true, the phase angle of the standing wave part in the center of the plasma is

$$\varphi(x=0) = \int_0^{x_0} k_x(x)\,dx \qquad (9)$$

or $\varphi(x=0) = k_x x_0$, if we assume a homogeneous plasma. This assumption should be well satisfied in our plasma, since according to Eq. (7 b, c) for our parameters the wavenumber is nearly independent of the density ($\omega_{pi}^2/\omega^2 \approx 100$).

Figure 7 shows a measurement of $\varphi(x=0)$ as a function of frequency, and for two different discharge currents. The solid lines are computed phases according to Eq. (9), assuming the waves are perpendicular ion acoustic waves satisfying Eq. (7 b), the electron temperature is taken to be 3 eV according to the measured value. The three lines are for different effective plasma radii and the best agreement in the slope is obtained for $x_0 = 2$ cm, which is a reasonable value when we consider the experimental density profile in Figure 8. However, although the slope agrees, there is still a considerable, rather constant phase difference between measured and the thus calculated phases $\varphi(x=0)$ which cannot be explained by merely assuming that the wave propagates oblique at an angle $\Theta < 90°$ rather than perpendicular so that $k_x = k \cdot \sin\Theta$. This means, that our explanation of the situation at hand is too crude, and it will be reexamined in the next section.

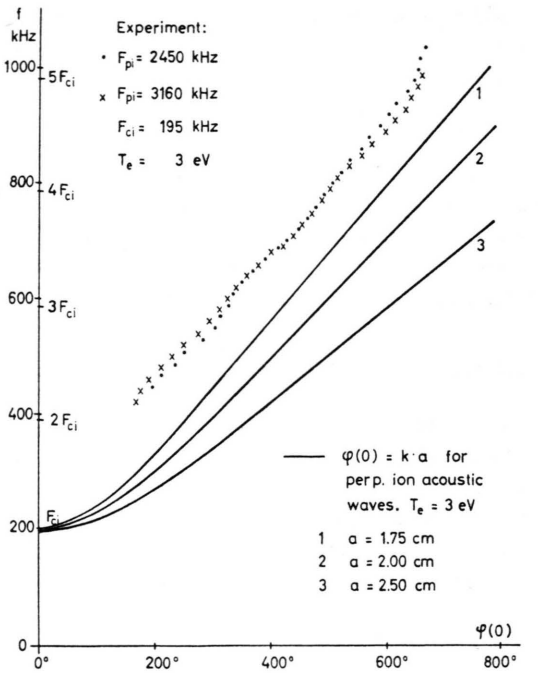

Fig. 7. Dots: experimentally determined phases $\varphi(x=0)$ compared to the perpendicular ion acoustic wave dispersion relation (solid lines, different effective plasma radii).

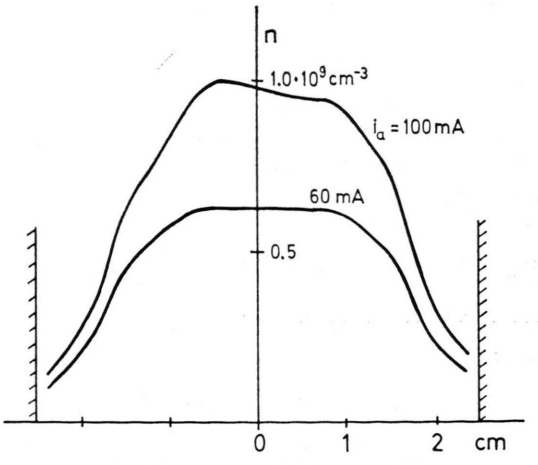

Fig. 8. Experimental density profile.

In addition we want to remark that we did not observe any effects due to the ion cyclotron harmonics. This is reasonable since in this kind of plasma we have $T_i \ll T_e$ and the gap which appears in the dispersion diagram below the harmonics is very narrow. Also we did not observe any resonances of the type of the Buchsbaum-Hasegava resonances [8] although we carefully looked for them by monitoring the r. f.-current flowing into the primary coil of the balanced exciter.

III. Grid Capacitor at Ion Wave Frequencies

To get an idea of what is going on we look at a grid capacitor, immersed in an infinite homogeneous plasma with cold ions ($\mu_i = 0$) and an infinite magnetic field for the electrons ($\omega_{ce} = \infty$, $\mu_e = 0$). However, the electrons can move freely along B_0 with their thermal velocity. The capacitor treated

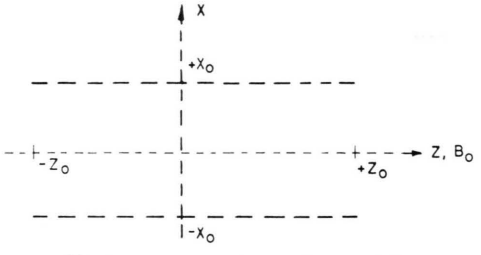

Fig. 9. − − − grid capacitor model.

here consists of a pair of grids, which carry an oscillating surface charge σ_0 producing a space charge, Figure 9,

$$\varrho_{ext}(x,z) = \sigma_0\big(-\delta(x+x_0)+\delta(x-x_0)\big)\cdot \cdot\begin{cases}0 & z<-z_0\,;\\ 1 & -z_0 \leqq z \leqq z_0\,;\\ 0 & +z_0<z\,.\end{cases} \tag{10}$$

It is assumed to be infinitely long in y-direction, so that $\partial/\partial y \equiv 0$. Then, from Poisson's equation we may derive a differential equation for the potential which after a Fourier transformation in z-direction reads:

$$\frac{\partial^2}{\partial x^2}\Phi(x,k_z) + k_x^2\,\Phi(x,k_z) = \frac{-\varrho_{ext}(x,k_z)}{\varepsilon_0 K_{xx}} \tag{11}$$

where k_x^2 is given by (8), $K_{xx} = 1 + \varkappa_{xxi}$, and $\varrho_{ext}(x,k_z)$ is the Fourier transform of $\varrho_{ext}(x,z)$

$$\varrho_{ext}(x,k_z) = \sigma_0\big(-\delta(x+x_0)+\delta(x-x_0)\big) \cdot 2\,z_0\,\frac{\sin k_z z_0}{k_z z_0} = f(x)\cdot\sigma(k_z)\,.$$

The solution to (11) valid between the two grids, is

$$\Phi(x,k_z) = -\frac{\exp\{-i k_x x_0\}}{k_x \varepsilon_0 K_{xx}}\,\sigma(k_z)\sin k_x x = \frac{\sigma(k_z)}{2\,i\,k_x\,\varepsilon_0 K_{xx}}\big(-\exp\{-i k_x(x+x_0)\} + \exp\{+i k_x(x-x_0)\}\big)\,. \tag{12}$$

This we recognize as the superposition of two waves travelling from the grids at $x = \pm x_0$ towards one-another.

The potential in real space is obtained by an inverse Fourier transform:

$$\Phi(x,z) = \frac{-2\,\sigma_0}{\pi\,\varepsilon_0 K_{xx}}\int_0^\infty \frac{\sin k_z z_0}{k_z} \cdot\exp\{-i k_x x_0\}\;\frac{\sin k_x x}{k_x}\cos k_z z\,\mathrm{d}k_z\,. \tag{13}$$

Here we see that in order to describe the r. f. potential correctly we have to integrate over all the obliquely propagating waves, which are excited by the grids with an amplitude according to the Fourier transform of their charge, $\sigma(k_z)$. Figure 10 shows this excitation spectrum. Also indicated are the regions where we may use the various approximations to the dispersion relation as discussed in the

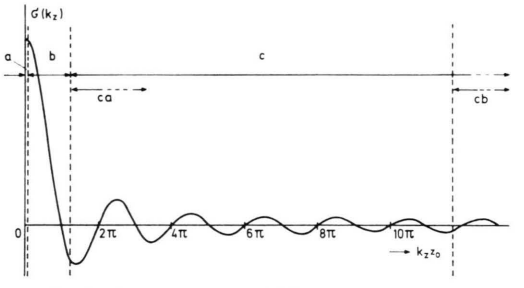

Fig. 10. Excitation spectrum $\sigma(k_z)$ in region a we may use Eq. (5 a), yielding the cold plasma potential, in region b we may use Eq. (8), in region c we may use Eq. (7 c), oblique ion acoustic waves, in region ca we may use Eq. (7 b) perpendicular ion acoustic waves, in region cb we get imaginary k_x, i. e. a high damping of the integrand in Equation (13).

beginning. Now we recognize that the crude model in Chapter II of a cold plasma potential and a superimposed perpendicular ion acoustic wave takes into account only two very limited regions, a and ca, of the excitation spectrum, while the major regions are neglected. Especially the region b gives a large complex contribution to the integral in Eq. (13) and thus will have a considerable influence on the phase of $\Phi(x,z)$ around $x = 0$.

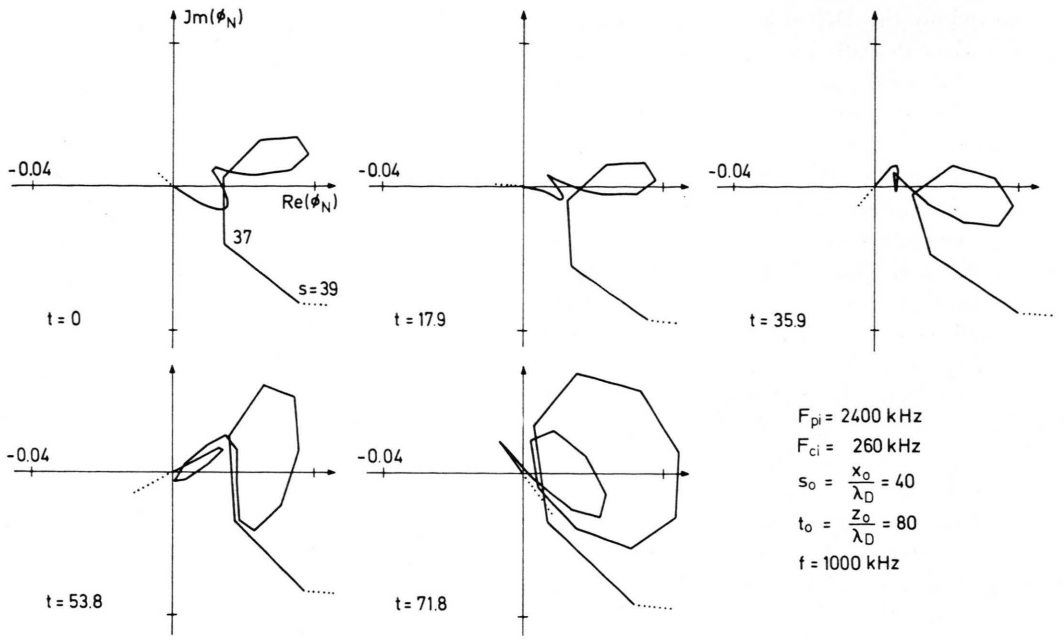

Fig. 11. Computed r. f. potentials $\Phi_N(s,t)$ in the complex plane for various positions $t=z/\lambda_D$ within the capacitor.

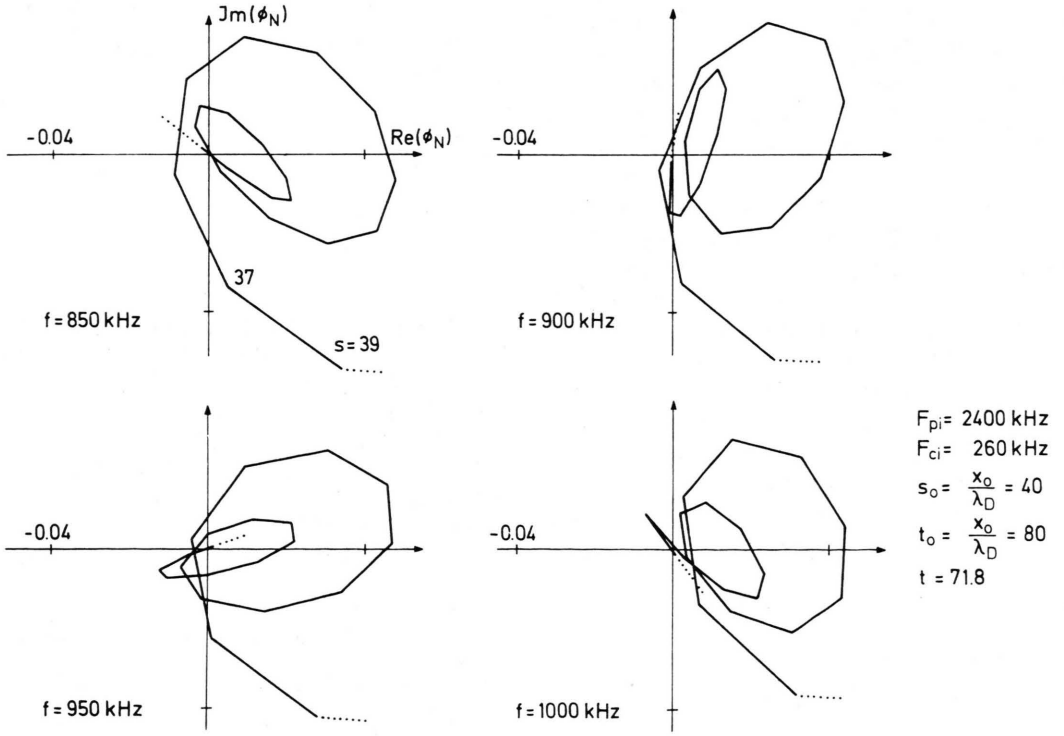

Fig. 12. Computed r. f. potentials $\Phi(s,t)$ in the complex plane for different frequencies, and $t=71.8$, i. e. near the edge of the capacitor.

In Fig. 11 we see a direct evaluation of Eq. (13) by means of a fast Fourier transform program, rigorously using Eq. (8) as dispersion relation over the whole spectral range. The coordinates x and z

are normalized to the Debey length, $s = x/\lambda_D$ and $t = z/\lambda_D$. For the calculation we took the dimensions of the capacitor grids as $s_0 = x_0/\lambda_D = 40$, and $t_0 = z_0/\lambda_D = 80$, in agreement with the experiment. There we had the probe at $z = 0$. The computed traces in Fig. 11 for $t = 0$, 17.9, 35.9, 53.8, however, don't look very similar to the measured ones. We even get opposite sense of rotation of the wave loops at $t = 35.9$ and 53.8, which seems very strange since we took $T_i = 0$ in the calculation and thus cannot get effects due to backward ion Bernstein waves. However, a pretty trace like those we measured is the one near the end of the capacitor at $t = 71.8$. How can we explain that? In Fig. 11 we can see that the phase of $\Phi(s, t)$ around $s = 0$ depends strongly on the position t along the capacitor. Computing $\Phi(t)$ for a constant value of s from Eq. (13), we see that we have not only perpendicularly propagating waves, but also parallel propagation with a wavelengths of $\lambda/\lambda_D \approx 15$, corresponding to the wavelength of parallel propagating ion acoustic waves. These require an electric field along the z-axis. In the experiment this field can, however, not develop along the probe. Therefore we don't see any wave coming from the side along the probe and thus it appears as if the probe were at the end of the capacitor (or as if the capacitor terminated at $x \approx 0$).

Figure 12 shows calculated potentials for various frequencies and $t = 71.8$, and we can see how here too the phase at $x = 0$ changes with frequency. We measure this phase angle as we do in the experiment and compare it with the phase that would result if the field were due to a superposition of a cold plasma field and perpendicularly propagating ion acoustic waves, which is $\varphi(x = 0) = k_x x_0$ with k_x out of Equation (7b). This is seen on Fig. 13 and we see that here too the actual phases are displaced by the same order of magnitude as has been experimentally observed in Figure 7.

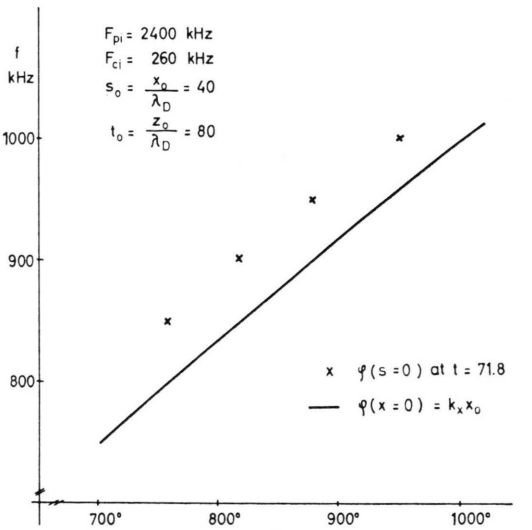

Fig. 13. Dots: Phases $\varphi(x = 0)$ as obtained from Fig. 10 compared to the perpendicular ion acoustic wave dispersion relation.

IV. Conclusion

This experiment shows that in an ion wave experiment we really have to consider the whole k_z-spectrum which is excited. The picture of a cold plasma field and one superimposed wave field is certainly wrong in most cases. Second, we need to think about the possibility of the probe shorting out electric fields and destroying the wave patterns, when evaluating probe measurements of electrostatic waves.

Acknowledgement

This experiment has been performed while I was on a research fellowship at the California Institute of Technology, Pasadena 91109, Ca., U.S.A. I gratefully acknowledge the many extensive discussions I had with Prof. R. W. Gould, and also the assistence from and the discussions with his students K. Burell, Ch. Moeller, and J. Wilgen. The computations of Eq. (13) with a fast Fourier transform program have been performed by A. Chang.

[1] M. Omura and H. Derfler, Stanford University, Report SU-IPR 156, 1967.
[2] T. H. Stix, The Theory of Plasma Waves, McGraw Hill, London 1962, Chapter 2.9.
[3] J. A. Hirose, I. Alexeff, and W. Jones, Phys. Fluids **13**, 2039 [1970].
[4] E. R. Ault and H. Ikezi, Phys. Fluids **13**, 2874 [1970].
[5] J. P. M. Schmitt, Phys. Fluids **15**, 2057 [1972].
[6] A. W. Trivelpiece and R. W. Gould, J. Appl. Phys. **30**, 1784 [1959].
[7] B. B. O'Brien, IEEE Trans. Instr. + Measurements IM-16, 124 [1967].
[8] S. J. Buchsbaum and A. Hasegawa, Phys. Rev. Lett. **12**, 685 [1964].